Preparation of Molecularly Imprinted Polymer Microspheres via Atom Transfer Radical Precipitation Polymerization

BAIYI ZU, GUOQING PAN, XIANZHI GUO, YING ZHANG, HUIQI ZHANG

Key Laboratory of Functional Polymer Materials, Ministry of Education, Department of Chemistry, Nankai University, Tianjin 300071, People's Republic of China

Received 26 November 2008; accepted 5 March 2009
DOI: 10.1002/pola.23389
Published online in Wiley InterScience (www.interscience.wiley.com).

ABSTRACT: The first combined use of atom transfer radical polymerization (ATRP) and precipitation polymerization in the molecular imprinting field is described. The utilized polymerization technique, namely atom transfer radical precipitation polymerization (ATRPP), provides MIP microspheres with obvious molecular imprinting effects towards the template, fast template binding kinetics and an appreciable selectivity over structurally related compounds. The living chain propagation mechanism in ATRPP results in MIP spherical particles with diameters (number-average diameter $D_n \approx 3$ μm) much larger than those prepared via traditional radical precipitation polymerization (TRPP). In addition, the MIP microspheres prepared via ATRPP have also proven to show significantly higher high-affinity binding site densities on their surfaces than the MIP generated via TRPP, while the binding association constants K_a and apparent maximum numbers N_{max} of the high-affinity sites as well as the specific template bindings are almost the same in the two cases. © 2009 Wiley Periodicals, Inc. J Polym Sci Part A: Polym Chem 47: 3257–3270, 2009

Keywords: atom transfer radical polymerization (ATRP); microsphere; molecular imprinting; precipitation polymerization; selectivity

INTRODUCTION

Molecular imprinting technique is a simple and efficient method for the preparation of synthetic polymers with tailor-made recognition sites for certain target molecules.[1–5] The resulting molecularly imprinted polymers (MIPs) have proven to show not only high specificity towards the template molecules but also favorable mechanical, thermal and chemical stability, which make MIPs very promising candidates for many applications, including chromatographic stationary-phase, solid-phase extraction, antibody mimics, biomimetic catalysis, sensors, organic synthesis, drug development and so on.[1–5]

The molecular imprinting process typically involves the copolymerization of a functional monomer and a crosslinking monomer in the presence of a template molecule in a suitable solvent. The functional monomer interacts with the template via noncovalent interactions (hydrogen bonds, ionic and hydrophobic interactions) to form a complex before the crosslinking reaction. After polymerization, the template is removed from the resulting polymer network, providing the molecularly imprinted binding sites (cavities) complementary to the shape, size and functionality of the template. Nowadays, MIPs are mostly prepared by using free radical polymerization mechanism due to its tolerance for a wide range of functional groups in the monomers and templates as

Correspondence to: H. Zhang (E-mail: zhanghuiqi@nankai.edu.cn)

Journal of Polymer Science: Part A: Polymer Chemistry, Vol. 47, 3257–3270 (2009)

well as its mild reaction conditions. However, traditional radical polymerization processes are usually rather difficult to control with regard to chain propagation and termination, which normally lead to polymer networks with heterogeneous structures.[6] The presence of heterogeneity within the network structures of the MIPs could have significant impact on the binding sites created inside them, which might be responsible for some of the inherent drawbacks of the MIPs such as the broad binding site heterogeneity and the relatively low affinity and selectivity. Therefore, it can be envisioned that the preparation of MIPs with homogeneous network structures will be of significant importance both for better understanding the structure-property relationship of the MIPs and for obtaining MIPs with improved binding properties. In this respect, controlled/"living" radical polymerization techniques (CRPs) are perfectly suited for this purpose. It has been well understood that the structural heterogeneity in the polymer networks generated by traditional radical polymerization is stemmed from the mismatch between the rapid chain growth and slow chain relaxation, which leads to the reduced reactivity of the pendant vinyl group and/or various cyclization reactions and the formation of heterogeneous polymer networks distributed with highly crosslinked microdomains.[6] In sharp contrast, CRPs are thermodynamically controlled processes with negligible chain termination and a more constant and much slower rate for the polymer chain growth, which dramatically improve the match in the chain growth and chain relaxation rates and thus lead to homogeneous polymer networks with a narrow distribution of the network chain length and a significantly lower crosslinking density in comparison with that of the crosslinked microdomains in the heterogeneous polymer networks (note that the crosslinking density in the MIPs prepared via CRPs should be still high enough to be able to stabilize the binding sites due to the use of large amounts of crosslinkers). So far, many different polymer networks with homogeneous structures have been prepared via CRPs.[6–11]

Since its first discovery in 1995,[12–14] atom transfer radical polymerization (ATRP) has rapidly attracted growing interest because of its versatility in the synthesis of polymers with predictable molecular weights, low polydispersities, and specific functionalities as well as its easy availability of many kinds of initiators, catalysts, and monomers.[15,16] It is based on a fast, dynamic equilibrium established between the dormant species (alkyl halides) and active species (radicals), with transition-metal complexes acting as reversible halogen atom transfer reagents [Scheme 1(a)], which keeps a very low radical concentration in the system and thus results in negligible radical termination and controlled polymerization.[15,16] The end groups of the polymers prepared via ATRP are defined by the utilized initiators. When an alkyl halide (or arenesulfonyl halide) is used as the initiator, the one end group of the obtained polymer chain is the alkyl (or arenesulfonyl) group of the initiator while the other end group is the halide. This characteristic makes the obtained polymers highly useful for further modification by using either standard organic procedures (e.g., nucleophilic substitution) or by their further reinitiation with the ATRP of other monomers.[17,18] So far, ATRP has been mostly utilized to prepare well-defined linear polymers. Recent years, however, have also witnessed an increasing interest in the use of ATRP for generating crosslinked polymers with homogeneous networks.[6,9,10]

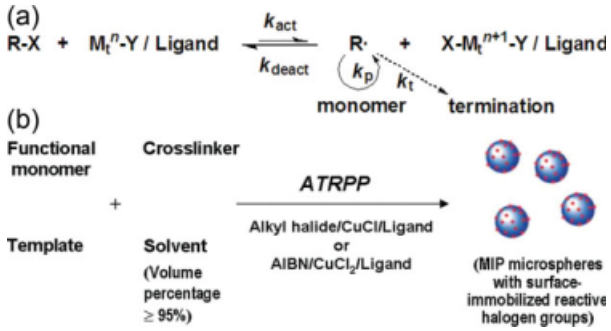

Scheme 1. The mechanism of ATRP (a) and schematic representation for the preparation of MIP microspheres via ATRPP (b).

Very recently, ATRP has also been applied in the molecular imprinting field for the generation of MIPs.[19–22] Husson and coworkers reported the successful molecular imprinting on the surfaces of gold-coated silica wafers[19,20] and silica gel[21] via ATRP. Yang and Wang's group described the controlled synthesis of MIP nanotube membranes by using surface-initiated ATRP.[22] The controllable nature of ATRP has proven to allow the growth of uniform MIP films with adjustable thicknesses, preventing diffusional mass transfer limitations from affecting the kinetic analysis.[19,21,22] Besides, relatively higher binding capacities have also been observed in some cases.[21,22] Based on these promising results, we can see that ATRP is of

great potential in the molecular imprinting field for the preparation of MIPs with tailor-made structures and improved binding properties. However, to our knowledge, its application has only been limited in the preparation of MIP films up to now. Therefore, it should be of great importance to extend the application of ATRP to the synthesis of MIPs with other different formats to show its versatility and general applicability.

Herein we present a general protocol for the direct preparation of functional MIP microspheres by atom transfer radical precipitation polymerization (ATRPP), a polymerization technique combining ATRP and precipitation polymerization [Scheme 1(b)]. Note that precipitation polymerization has proven versatile for preparing MIP micro/submicrospheres because of its easy operation and no need for any surfactant or stabilizer,[23–26] but only traditional radical precipitation polymerization (TRPP) has been utilized up to now. To our knowledge, this is the first report on the application of ATRPP in the molecular imprinting field. It should be mentioned here that a combined use of ATRP and precipitation polymerization has been reported for the preparation of linear polymers,[27] but it has never been utilized for preparing crosslinked polymer microspheres. The introduction of ATRP mechanism into precipitation polymerization will lead to MIP microspheres with reactive halogen groups on their surfaces, which are highly useful for their further surface modification (leading to their better compatibility with different solvent systems) either by standard organic procedures or by surface-initiated ATRP. The chemical structures, particle morphology, size and size distribution, template rebinding properties, surface areas and the selectivity of the resulted MIP microspheres were characterized in detail, and they were also compared with those of the MIP particles prepared via TRPP to get a better understanding on their structure-property relationship. In addition, the general applicability of ATRPP in the molecular imprinting filed was also demonstrated by the preparation of MIP microspheres with other templates.

EXPERIMENTAL

Materials

4-Vinylpyridine (4-VP, Alfa Aesar, 96%) and ethylene glycol dimethacrylate (EGDMA, Alfa Aesar, 98%) were purified by distillation under vacuum.

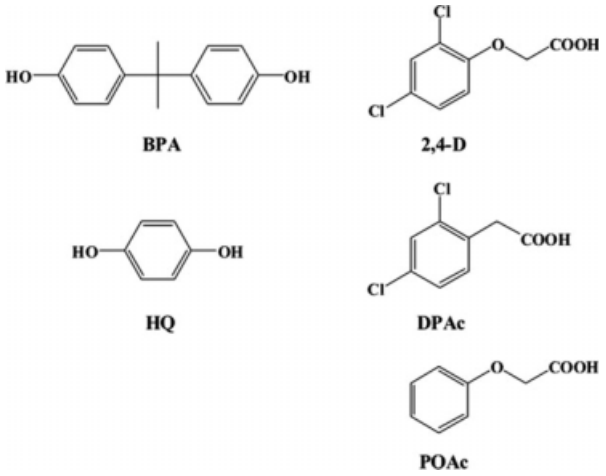

Scheme 2. The chemical structures of the template molecules and their related test compounds.

Acetonitrile [Jiangtian Chemical, China, analytical grade (AR)] was distilled over CaH_2 before use. Methanol (Jiangtian Chemical, AR) was distilled before use. Azobisisobutyronitrile (AIBN, Chemical Plant of Nankai University, AR) was recrystallized from ethanol. Copper(I) chloride (CuCl, Jiangtian Chemical, China, AR) was purified following a reported procedure.[28] Tris[2-(dimethylamino)ethyl]amine (Me_6TREN) was prepared by a one-step synthesis procedure from commercially available tris(2-aminoethyl)amine (TREN, Acros, 97%) according to a reported procedure.[29] Bisphenol A (BPA, Guangfu Fine Chemicals, China, AR), hydroquinone (HQ, North Tianyi Chemical Company, China, AR), 2,4-dichlorophenoxyacetic acid (2,4-D, Alfa Aesar, 98%), 2,4-dichlorophenylacetic acid (DPAc, Acros, 99%), phenoxyacetic acid (POAc, Acros, 98+%) *N*,*N*,*N*′,*N*″,*N*″-pentamethyldiethylenetriamine (PMDETA, Aldrich, 99%), anhydrous copper(II) chloride ($CuCl_2$, Alfa Aesar, 98%) and ethyl 2-chloropropionate (Alfa Aesar, 97%) were used as received. The chemical structures of BPA, HQ, 2,4-D, DPAc and POAc are shown in Scheme 2.

Preparation of a BPA Imprinted Polymer (BPA-MIP) and Its Corresponding Nonimprinted Polymer (NIP) by Normal ATRPP

The BPA-MIP was prepared via normal ATRPP according to the following procedure: To a 100 mL round-bottom flask, CuCl (0.0052 g, 0.0525 mmol) was added to a solution of BPA (0.3424 g, 1.4998 mmol), 4-VP (0.1577 g, 1.4999 mmol) and EGDMA (0.8919 g, 4.5045 mmol) in dried

acetonitrile (30 mL). The reaction mixture was purged with argon for 15 min and then PMDETA (0.0182 g, 0.1050mmol) was added. After another 15 min of argon bubbling, ethyl 2-chloropropionate (0.0072 g, 0.0527 mmol) was added into the system. The flask was then sealed and immersed into a thermostated oil bath at 60 °C for 24 h. The polymer particles collected by filtration were purified through Soxhlet extraction with methanol/acetic acid (9/1 v/v, 48 h) and acetonitrile (24 h) successively to remove both the template and copper catalyst, which were then dried at 40 °C under vacuum overnight to provide the desired MIP (yield: 62%).

The NIP was prepared and purified under the identical conditions except that the template was omitted (yield: 60%).

Preparation of a 2,4-D Imprinted Polymer (2,4-D-MIP) and Its NIP by Normal ATRPP

The 2,4-D-MIP was prepared via normal ATRPP according to the following procedure: To a 100 mL round-bottom flask, CuCl (0.0069 g, 0.0697 mmol) was added to a solution of 2,4-D (0.1105 g, 0.4999 mmol), 4-VP (0.2103 g, 2.0001 mmol) and EGDMA (1.1893 g, 6.0066 mmol) in dried acetonitrile (30 mL). The reaction mixture was purged with argon for 15 min and then Me_6TREN (0.0484 g, 0.2101 mmol) was added. After another 15 min of argon bubbling, ethyl 2-chloropropionate (0.0096 g, 0.0703 mmol) was added into the system. The flask was then sealed and immersed into a thermostated oil bath at 60 °C for 24 h. The polymer particles collected by filtration were purified through Soxhlet extraction with methanol/acetic acid (9/1 v/v, 48 h) and acetonitrile (24 h) successively to remove both the template and copper catalyst and then dried at 40 °C under vacuum overnight to provide the desired MIP (yield: 35%).

The corresponding NIP was prepared and purified under the identical conditions except that the template was omitted (yield: 48%).

Preparation of the MIPs (Template: BPA or 2,4-D)/NIPs by Reverse ATRPP

The MIPs (template: BPA or 2,4-D)/NIPs were prepared by reverse ATRPP following a similar procedure as normal ATRPP except that CuCl and ethyl 2-chloropropionate were replaced by $CuCl_2$ and AIBN, respectively. The reaction time was changed to 48 h for the system with BPA as the template, while it was still kept at 24 h for the system with 2,4-D as the template. The yields of the MIP prepared with BPA as the template and its corresponding NIP were 85 and 81%, respectively, and those of the MIP prepared with 2,4-D as the template and its NIP were 59 and 72%, respectively.

Preparation of the MIPs (Template: BPA or 2,4-D)/NIPs by TRPP

The MIPs (template: BPA or 2,4-D)/NIPs were prepared by TRPP following a similar procedure as normal ATRPP except that AIBN was used to replace ethyl 2-chloropropionate/CuCl/ligand (PMDETA or Me_6TREN). The yields of the MIP prepared with BPA as the template and its corresponding NIP were 76 and 79%, respectively, and those of the MIP prepared with 2,4-D as the template and its NIP were 86 and 64%, respectively.

Characterizations

Fourier Transform Infrared (FTIR) spectra of the MIPs were measured with a Nicolet Magna-560 FTIR spectrometer.

The elemental analyses of the MIPs/NIPs were carried out by using Elementar Vario EL (Germany) to determine their chemical compositions and crosslinking densities. If we assume that the obtained MIPs/NIPs contain x moles of the bonded 4-VP unit (molecular formula: C_7H_7N) and y moles of the bonded EGDMA unit (molecular formula: $C_{10}H_{14}O_4$), the following equations can be obtained for the weight fractions of carbon (C_C) and nitrogen (C_N):

$$C_C = (7x + 10y)M_C/(xM_{4\text{-VP}} + yM_{EGDMA}),$$

$$C_N = xM_N/(xM_{4\text{-VP}} + yM_{EGDMA})$$

where M_C is the atomic weight of carbon, M_N the atomic weight of nitrogen, $M_{4\text{-VP}}$ the molecular weight of 4-VP, and M_{EGDMA} the molecular weight of EGDMA. The molar fractions of the bonded EGDMA unit in the MIPs/NIPs (i.e., $y/(x + y)$, which can also be utilized to express the crosslinking densities of the MIPs/NIPs) can thus be obtained by introducing C_C and C_N values (determined by the elemental analysis) into the above two equations.

The particle morphology, size and size distribution of the MIPs/NIPs were determined with a scanning electron microscope (SEM, Shimadzu SS-550). All of the SEM size data reflect the

averages about 100 particles each, which are calculated by the following formulas:

$$U = D_w/D_n;$$

$$D_n = \sum_{i=1}^{k} n_i D_i \Big/ \sum_{i=1}^{k} n_i; \quad D_w = \sum_{i=1}^{k} n_i D_i^4 \Big/ \sum_{i=1}^{k} n_i D_i^3$$

where U is the polydispersity index, D_n the number-average diameter, D_w the weight-average diameter, N the total number of the measured particles, and D_i the particle diameters of the determined microspheres.

Surface area analyses were performed by nitrogen sorption porosimetry on a TriStar3000 Surface Area Analyzer (America Micromeritics Instrument Corp). Before the measurements, the MIPs/NIPs were firstly degassed at 100 °C under high vacuum for 10 h. The surface areas of the degassed MIP microspheres were then evaluated by using the Brunauer-Emett-Teller (BET) method.

The template concentrations were quantified with a high-performance liquid chromatography (HPLC, Scientific System) with a UV-vis detector. The mobile phases (flow rates: 1 mL/min) used for the determination of BPA and 2,4-D are a mixture of acetonitrile and water (6/4 v/v) and a mixture of methanol and 0.5% aqueous solution of acetic acid (4/1 v/v), respectively.

Binding kinetics of the template molecule BPA with the MIPs/NIPs prepared via different synthetic approaches were evaluated by batch adsorption experiments, where 10 mg of MIPs/NIPs were incubated with a solution of BPA (1 mL, 0.0438 mM) at ambient temperature for different times. After centrifugation, the amounts of the template remaining in the supernatants (expressed as F) were determined by HPLC and those bound to the MIPs/NIPs (B) could thus be obtained by subtracting F from the initial template concentration.

Equilibrium binding experiments (or saturation binding experiments) were carried out by incubating a BPA solution in acetonitrile (1 mL, 0.0438 mM) or a 2,4-D solution in acetonitrile (1 mL, 0.08 mM) with different amounts of MIPs/NIPs for 24 h, when the binding equilibriums with MIPs/NIPs were established and the binding capacities of the MIPs/NIPs reached their maximums. The incubating temperatures for the BPA and 2,4-D systems were 25 and 22 °C, respectively. The amounts of the templates bound to the MIPs/NIPs were then quantified with HPLC.

Binding isotherms of the MIPs were studied with Scatchard analysis:[30] BPA-MIP particles (5 mg) were incubated with a series of BPA solution in acetonitrile (C = 0.04–1.2 mM) at 25 °C for 24 h. After centrifugation, the amounts of the template bound to the MIPs (B) were determined by HPLC. The Scatchard equation used is $B/F = (N_{max} - B)K_a$, where K_a and N_{max} represent the binding association constant and apparent maximum number of the binding sites, respectively.

The binding selectivity of the MIPs was evaluated by measuring their competitive binding capacities towards the templates and their structurally related compounds as follows: (1) 16 mg of BPA-MIP particles were incubated with 1 mL of a mixed solution of BPA and HQ in acetonitrile (with their concentrations being the same, $C_{BPA\ or\ HQ}$ = 0.0438 mM) at 24 °C for 24 h, the amounts of BPA and its related compound bound to the MIPs were then quantified by HPLC; (2) 10 mg of 2,4-D-MIP particles were incubated with 1 mL of a mixed solution of 2,4-D, DPAc and POAc in acetonitrile (with their concentrations being the same, C = 0.08 mM) at 24 °C for 6 h, the amounts of 2,4-D and its related compounds bound to the MIPs were then quantified by HPLC.

All the above binding analyses were performed in duplicate and the mean values were used.

RESULTS AND DISCUSSION

Over the past few years, we have been working in the field of molecular imprinting[5,31,32] and ATRP.[17,33,34] The present contribution is aiming to combine the above two fields together and will mainly focus on two aspects, that is, to check whether ATRPP can be used to prepare MIP microspheres as a new polymerization technique for molecular imprinting and whether the resulted MIPs have some improved properties in comparison with those prepared via TRPP. This study will not only extend the application area of ATRP in the molecular imprinting field, but also lead to an in-depth understanding of the structure-property relationship of the MIPs prepared via different approaches.

So far, precipitation polymerization has proven to be one of the most attractive and reliable methods available for the easy preparation of MIP spherical particles with a diameter ranging from one to a few hundreds of nanometers to several micrometers.[23–26] It involves the polymerization of a functional monomer with a crosslinker in the

presence of a template under dilution conditions in a suitable solvent (typically 95% of the total reaction volumes) in the absence of any surfactant or stabilizer. The polymer beads formed in this way are protected from aggregation during polymerization by their crosslinked surfaces and are completely surfactant free. In comparison with the MIPs prepared via conventional imprinting approach (i.e., "bulk" polymerization), which are normally irregular particles with different sizes in the range of 5–100 μm after the time-consuming grinding of the generated porous monolith and the subsequent sieving, the MIP spherical particles generated via precipitation polymerization are highly desirable for such applications as homogeneous binding assays, HPLC stationary phases, solid-phase extraction and so on. In addition, these MIP spherical particles have also proven to show faster binding kinetics for the target analytes due to their small particle size and better accessibility of the binding sites in comparison with MIPs prepared via conventional imprinting method.[26] Based on the above statements, we can conclude that precipitation polymerization has many advantages over the conventional molecular imprinting approach and the combined use of precipitation polymerization with ATRP will further increase its versatility by providing functionalized MIP spherical particles.

Since MIPs are mostly prepared via noncovalent molecular imprinting technique nowadays due to its flexibility in preparation as well as its versatility in generating MIPs with high specificity and fast rebinding kinetics, a model noncovalent molecular imprinting system was chosen here to show the proof-of-principle, which utilized 4-VP, BPA, EGDMA and acetonitrile as the functional monomer, template, crosslinker and porogenic solvent, respectively. Note that all of the above reactants are compatible with both ATRP and molecular imprinting processes and 4-VP can form hydrogen bonding interaction with BPA in acetonitrile.

According to their different initiating species used, two kinds of ATRP processes are available, which are normal ATRP and reverse ATRP, respectively.[15] In the normal ATRP system, the initiating radicals are stemmed from the reaction between an alkyl halide and a transition metal complex in its lower oxidation state (e.g., Cu(I)/Ligand); while in the reverse ATRP system, conventional radical initiators (e.g., AIBN) are employed to generate primary radicals in the beginning of the polymerization, which are then deactivated by a transition-metal complex in its higher oxidation state (e.g., Cu(II)/ligand). In both systems, the equilibrium between the dormant species (alkyl halides) and active species (radicals) can be quickly established soon after the polymerization starts [Scheme 1(a)]. In this work, both normal ATRPP and reverse ATRPP were tried to prepare MIP microspheres, where a reactant combination of BPA/4-VP/EGDMA/ethyl 2-chloropropionate/CuCl/PMDETA (15/15/45/0.525/0.525/1.05, molar ratio) and BPA/4-VP/EGDMA/AIBN/$CuCl_2$/PMDETA (15/15/45/0.525/0.525/1.05, molar ratio) was utilized, respectively. For comparison, TRPP was also performed to prepare MIP particles by using BPA/4-VP/EGDMA/AIBN (15/15/45/0.525, molar ratio). In all cases, the molar ratio of BPA to 4-VP was chosen as 1, following a previously optimized recipe.[35,36] It is worth mentioning here that this molar ratio of BPA to 4-VP is much higher than that used in a normal molecular imprinting system, where an excess of functional monomers usually needs to be added into the system to shift the equilibrium towards complex formation. This might be attributed to the characteristics of precipitation polymerization, where very large amounts of porogenic solvents (typically 95% of the total reaction volumes) are normally used, which leads to most of the template dissolving into the porogenic solvents instead of interacting with the functional monomers to form prepolymerization complex.[23–26] Therefore, increasing the amount of template would be necessary to improve the formation of prepolymerization complex as well as the imprinting efficiency.[36,37] As references, the corresponding NIP particles were also prepared similarly by omitting the template in the reaction systems. All the reactions were performed at 60 °C in 30 mL of acetonitrile with its volume percentage being 97%. The resulted polymer particles were thoroughly purified through Soxhlet extraction, leading to white MIPs/NIPs with their yields ranging from 60 to 85%.

The obtained MIP particles were firstly characterized with FTIR. It can be seen clearly that the MIPs prepared via different approaches have rather similar IR spectra (Fig. 1). The presence of three significant peaks around 1728 (C=O stretching), 1250 and 1155 cm^{-1} (C—O—C stretching) supports the existence of poly(EGDMA) in the obtained MIPs. The characteristic peaks corresponding to the C=N stretching (1600 and 1558 cm^{-1}) and C=C stretching (1456 cm^{-1}) in the pyridine rings can also be observed in the spectra of

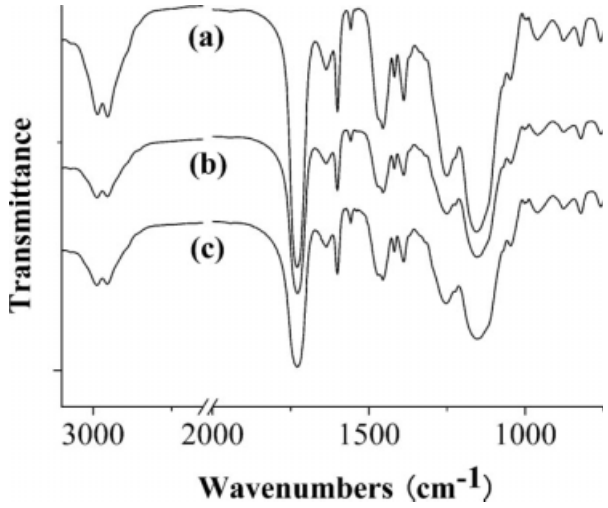

Figure 1. FTIR spectra of the MIPs prepared with BPA as the template via TRPP (a), normal ATRPP (b), and reverse ATRPP (c).

the MIPs, revealing that poly(4-VP) is also present in the MIPs. Furthermore, the presence of small peaks around 1637 cm^{-1} (corresponding to the C=C stretching mode) demonstrated that less than 100% of the bonded EGDMA molecules are crosslinked in the MIPs.[38]

The MIPs/NIPs were then studied with elemental analysis to determine their chemical compositions, from which the crosslinking densities of the MIPs/NIPs are readily available because they can be simply expressed by the molar fractions of the bonded EGDMA unit in the obtained polymers. Table 1 shows that the molar fractions of the bonded EGDMA unit in all the MIPs/NIPs prepared via different synthetic approaches are lower than that of EGDMA in the initial comonomer mixture (75%), suggesting that 4-VP is more reactive than EGDMA in the studied reaction systems. In addition, the MIPs/NIPs have proven to show crosslinking densities in the range of 61–69%, which are high enough for stabilizing the shapes of the imprinted cavities.

The particle morphology, size and size distribution of the obtained MIPs and NIPs were characterized with SEM (Fig. 2). Figure 2(a,b) show that TRPP provides MIP and NIP submicrospheres with a diameter of about 200–430 nm, which is comparable with the previous report.[23] The number-average diameters (D_n) of the MIP and NIP spherical particles prepared via TRPP are 307 and 329 nm, respectively, and they have a polydispersity index (U) of 1.17 and 1.13, respectively. In comparison, both normal and reverse ATRPP provide MIP and NIP microspheres with much larger diameters (ca. 2–5 μm) [Fig. 2(c–f)]. The D_n values of both the MIP and NIP spherical particles prepared via normal ATRPP are 3.20 and 3.04 μm, respectively, and they have a U value of 1.19 and 1.22, respectively. The D_n values of both the MIP and NIP spherical particles prepared via reverse ATRPP are 3.58 and 3.28 μm, respectively, and they have a U value of 1.27 and 1.20, respectively.

Table 1. Chemical Compositions and Equilibrium Binding Properties of the MIPs (Template: BPA) and NIPs Prepared via Different Synthetic Approaches as Well as Their Binding Parameters Obtained From Scatchard Analysis

Synthetic Approach	Chemical Composition (%)[a]	Binding Properties (%)		High-Affinity Sites[d]	
		Template Binding[b]	Specific Binding[c]	K_a (M^{-1}) $\times 10^{-4}$	N_{max} (μmol/g)
TRPP-MIP	69	24	9	1.14	3.3
TRPP-NIP	66	15			
Normal ATRPP-MIP	61	30	10	1.06	3.9
Normal ATRPP-NIP	63	20			
Reverse ATRPP-MIP	64	28	10	1.02	3.7
Reverse ATRPP-NIP	63	18			

[a] The molar fractions of the bonded EGDMA unit in the MIPs/NIPs as determined by the elemental analysis, which can be utilized to express the crosslinking densities of the MIPs/NIPs.

[b] Sixteen milligram of MIPs and NIPs were incubated with a BPA solution (1 mL, C = 0.0483 mM) at 25 °C for 24 h.

[c] Specific binding is defined as the deference in BPA adsorption between MIP and NIP.

[d] K_a and N_{max} represent the binding association constant and apparent maximum number of the binding sites, respectively.

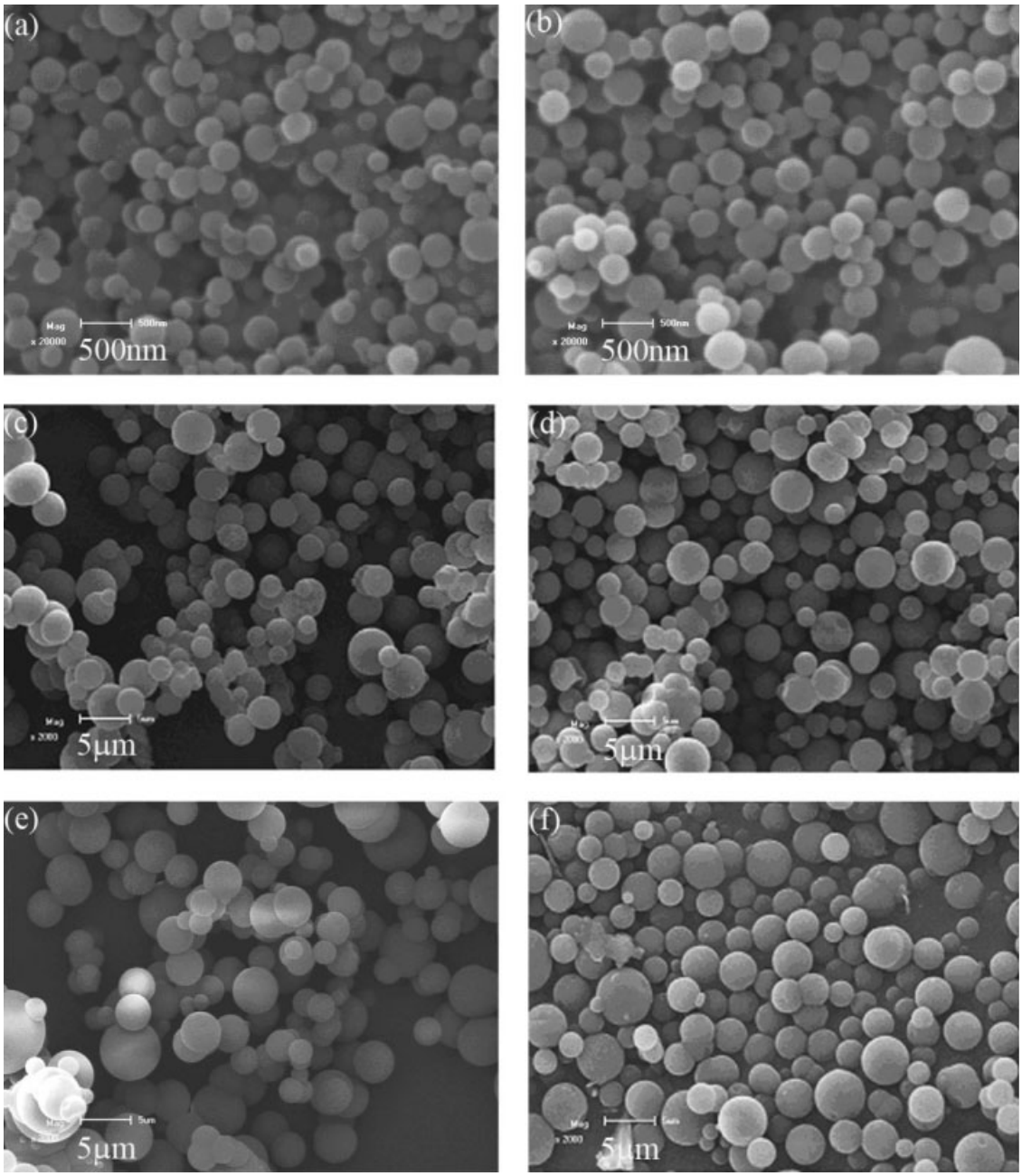

Figure 2. Scanning electron micrographs of the MIPs (template: BPA) (a,c,e) and NIPs (b,d,f) prepared via TRPP (a,b), normal ATRPP (c,d) and reverse ATRPP (e,f), respectively.

It can be seen clearly that the diameters of the MIP and NIP spherical particles prepared via both normal and reverse ATRPP are about 10 times larger than those prepared via TRPP, suggesting that the combined use of ATRP and precipitation polymerization has a significant impact on the particle sizes of the obtained MIPs/NIPs. This may not be surprising given that different polymerization mechanisms are involved in the two systems. The living nature of ATRPP might somehow influence both the formation of the particle nucleis in the solutions and their growth processes,[39] thus leading to larger spherical particles. A detailed study on the mechanism of ATRPP is under way and the results will be included in a forthcoming article.

It should be mentioned here that although TRPP has been widely utilized for the preparation

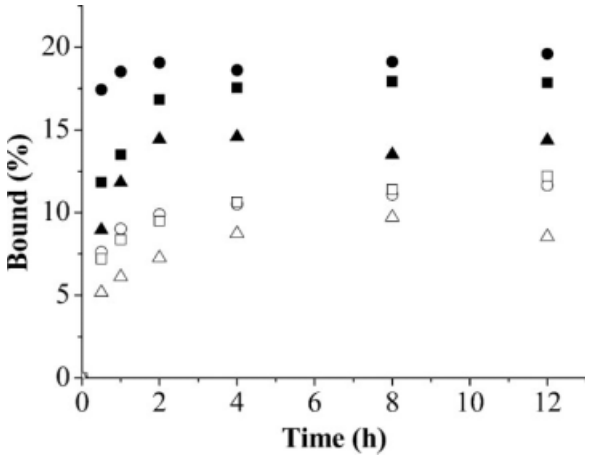

Figure 3. Binding kinetics of BPA on the MIPs (with BPA as the template, filled symbols) and NIPs (open symbols) prepared via TRPP (triangle), normal ATRPP (cycle) and reverse ATRPP (square), respectively. Ten milligram of MIPs and NIPs were incubated with a solution of BPA (1 mL, 0.0438 mM) at 25 °C for different times.

of MIP spherical particles for a wide range of templates, only those with relatively smaller diameters (<1 μm) have been obtained in most cases.[23,24] While these small MIP spherical particles are very suitable for such applications as homogeneous binding assays, microfluidic separation modules, and recognition layers on sensor surfaces, many other applications such as the stationary phases in HPLC require relatively larger MIP microspheres (1.5–5 μm).[24,25] Therefore, recent years have witnessed significant efforts being devoted for this purpose. Recently, MIP microspheres with a diameter of about 5 μm have been obtained by carefully matching the solubility parameters of the developing polymer network to that of the porogenic solvent(s), where divinylbenzene (DVB) and a mixture of acetronitrile and toluene were utilized as the crosslinker and the porogenic solvent, respectively.[24] MIP microspheres with relatively larger diameters (2.4 μm) have also been prepared by using DVB as the crosslinker by Ye and coworkers.[25] To our knowledge, however, the simultaneous use of pure acetronitrile as the porogenic solvent and EGDMA as the crosslinker has seldom led to the MIP microspheres with a diameter larger than 3 μm up to now. In this sense, our approach described here seems to be very promising for the easy preparation of MIP microspheres with relatively larger diameters (~3 μm).

The binding kinetics of the template molecule BPA with the MIPs and NIPs prepared via TRPP, normal ATRPP and reverse ATRPP were evaluated by batch adsorption experiments. Figure 3 shows the adsorption uptake of the polymers versus the incubation time. It can be seen clearly that all the MIPs prepared via different synthetic approaches reach their binding equilibriums at a time of about 2 h, indicating quite fast binding processes. In comparison, a relatively longer time (≥4 h) is required for all the NIPs to reach their binding equilibriums. In addition, the equilibrium loading capacities for the MIPs prepared via both normal and reverse ATRPP have proven to be rather similar, but they are higher than that for the MIP prepared via TRPP. Similar phenomena were also observed for their corresponding NIPs.

Equilibrium binding experiments were then performed to study the rebinding properties of the MIPs and NIPs. Figure 4 shows that the MIP particles prepared via both (normal and reverse) ATRPP and TRPP bind more template than their corresponding NIPs. For example, in a dilute solution of BPA in acetonitrile, while 16 mg of the imprinted spherical particles prepared via normal ATRPP, reverse ATRPP and TRPP bound 30, 28, and 24% of the template, respectively, an equivalent amount of the corresponding controls bound only 20, 18, and 15%, respectively, (Table 1). These results confirmed the presence of selective binding sites created by the template in the obtained MIPs and thus the successful molecular imprinting processes in both ATRPP and TRPP. In

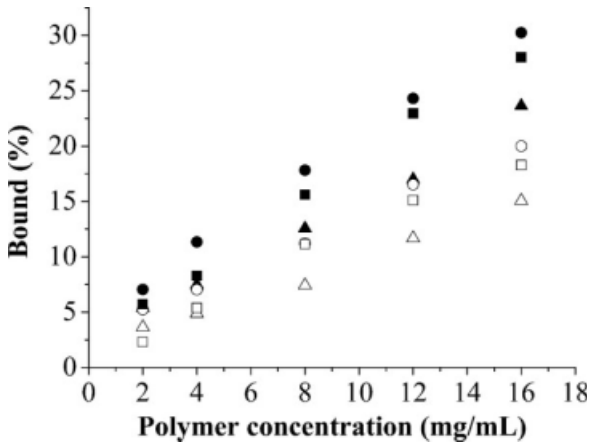

Figure 4. Equilibrium binding of BPA (C = 0.0438 mM) on different amounts of MIPs (template: BPA, filled symbols) and NIPs (open symbols) prepared via TRPP (triangle), normal ATRPP (cycle) and reverse ATRPP (square), respectively.

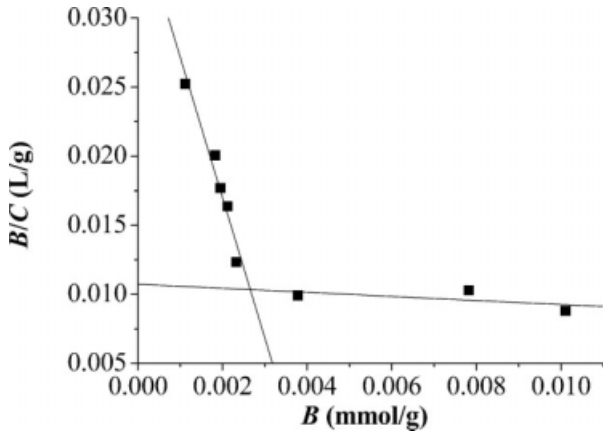

Figure 5. Scatchard plot of the MIP prepared via reverse ATRPP with BPA as the template.

addition, the MIPs prepared via both normal and reverse ATRPP proved to bind more BPA than that prepared via TRPP, indicating that improved binding capacities were achieved in the MIPs prepared via ATRPP. However, a further study revealed that the MIPs prepared via both ATRPP and TRPP showed quite similar specific template bindings if we simply define the specific binding as the deference in BPA adsorption between the MIP and NIP (Table 1),[40,41] which suggests that the increased binding capacities of the MIPs prepared via ATRPP are mainly stemmed from their relatively higher nonspecific binding.

To get more insight into the binding characteristics of the MIPs prepared via different synthetic approaches, they were further studied with Scatchard analysis. The Scatchard plot of one representative MIP (prepared via reverse ATRPP) is shown in Figure 5. The results showed that the Scatchard plots of all the MIPs could be fitted into two straight lines, suggesting that the binding sites in the MIPs prepared via both ATRPP and TRPP are heterogeneous and their affinities can be approximated by two binding association constants (K_a) corresponding to the high- and low-affinity sites, as usually observed for the MIPs prepared via the noncovalent molecular imprinting approach.[42] We are particularly interested in the high-affinity sites because they are mainly responsible for the specific binding of the MIPs. Table 1 shows that all the MIPs have rather similar K_a and N_{max} values for the high-affinity sites, which agree well with their similar specific template binding properties.

It is known that the surface area properties of the MIPs have significant influence on their binding properties. Therefore, the surface areas of the obtained MIP particles were also characterized by performing nitrogen adsorption experiments using the BET model. Li and Stöver disclosed that the microspheres prepared via precipitation polymerization in the pure acetonitrile exhibited small surface areas (ca. 9 m^2/g).[39] Lu and coworkers also reported a rather small surface areas (<6 m^2/g) for the MIPs prepared via TRPP using BPA as the template and acetonitrile as the porogenic solvent.[36] In our case, the surface areas of the MIP particles prepared via both normal and reverse ATRPP in acetonitrile were found to be too small to be accurately determined. In comparison, the MIP particles prepared via TRPP showed relatively larger surface areas (26.7 m^2/g). Based on these surface area results and the above-described almost similar apparent numbers N_{max} of high-affinity sites in the MIPs prepared via different synthetic approaches (Table 1), we can conclude that the high-affinity site densities ($\rho = N_{max}$/surface areas) on the surfaces of the MIP particles prepared via both normal and reverse ATRPP should be much higher than that of the MIP prepared via TRPP. This is likely to be due to the unique living chain propagation mechanism in ATRPP, which allows a more constant rate for the polymer chain growth, thus resulting in an increased structural homogeneity and improved stability and integrity of the binding sites.

The binding selectivity of the MIPs was studied by measuring their competitive binding capacities towards BPA and a related phenolic compound HQ, which has the same numbers of hydroxyl group as BPA but differs in their backbones (Scheme 2). As shown in Figure 6, besides binding

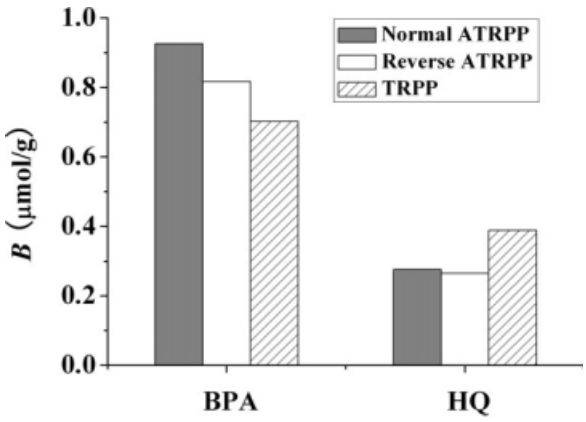

Figure 6. Selective binding of the MIPs (BPA as the template) prepared via different synthetic approaches towards BPA and HQ in their mixed solution in acetonitrile ($C_{BPA\ or\ HQ} = 0.0438$ mM), respectively.

BPA, the MIPs prepared via both ATRPP and TRPP also adsorbed HQ, suggesting the presence of certain cross-binding reactivity. Nevertheless, the binding of the MIPs towards HQ was obviously lower than that of the MIPs towards BPA, demonstrating the high selectivity of the MIPs towards BPA. This is easily understandable because the binding sites in the MIPs are complementary to the template in shape, size and chemical functionality. It is worth mentioning here that while the presence of certain cross-binding reactivity in the MIPs might be undesirable for such applications as sensors, this could actually be an advantage in sample treatment because different kinds of phenolic compounds could also be removed or enriched efficiently.

Based on the above results, we can make a close comparison between the MIPs prepared via different approaches. Previous reports have shown that the application of CRPs in molecular imprinting could have rather different effects on the resulted MIPs.[21,22,40,41,43] In certain cases, the MIPs prepared via CRPs showed improved binding properties such as faster binding kinetics,[21] higher binding capacities,[21,22,40,43] and larger binding association constants,[40] while in some other cases, the binding properties of the MIPs prepared via CRP appeared very similar to those of the MIPs prepared via conventional approaches.[41] In this study, we found out that both TRPP and ATRPP could provide MIP spherical particles with obvious molecular imprinting effects towards the template, fast template binding kinetics and an appreciable selectivity over its structurally related compound. In addition, the living chain propagation mechanism in ATRPP resulted in MIP spherical particles with diameters (number-average diameter $D_n \approx 3$ μm) much larger than those prepared via TRPP. Furthermore, the MIP microspheres prepared via ATRPP have also proven to show significantly higher high-affinity site densities on their surfaces than the MIP prepared via TRPP, while the binding association constants K_a and apparent maximum numbers N_{max} of the high-affinity sites as well as the specific template bindings are almost the same in the two cases.

To show the general applicability of ATRPP in the molecular imprinting field, we also tried to prepare 2,4-D imprinted microspheres via ATRPP. 2,4-D is a widely used herbicide and it contains a carboxyl functional group (Scheme 2). Note that both the 2,4-D imprinted polymer monolith and submicrospheres have previously been prepared via traditional free radical bulk polymerization[44] and precipitation polymerization,[37] respectively, where 4-VP was utilized as the functional monomer to form interaction with 2,4-D. In our study, 4-VP, EGDMA and acetonitrile were chosen as the functional monomer, crosslinker and porogenic solvent, respectively. The utilized reactant combinations and their compositions were 2,4-D/4-VP/EGDMA/ethyl 2-chloropropionate/CuCl/Me_6TREN (1/4/12/0.14/0.14/0.42, molar ratio) and 2,4-D/4-VP/EGDMA/AIBN/$CuCl_2$/Me_6TREN (1/4/12/0.14/0.14/0.42, molar ratio) for the normal and reverse ATRPP, respectively. The use of Me_6TREN instead of PMDETA as the ligand in these systems could be ascribed to its stronger interaction with copper catalyst than PMDETA, which was expected to result in better catalytic stability and activity in the presence of the acidic template. As references, the corresponding NIPs were also prepared similarly by omitting the template in the reaction systems. All the reactions were carried out at 60 °C in acetonitrile with its volume percentage being about 96%. The purified MIPs and NIPs were white polymer powders with their yields ranging from 35 to 86%.

Figure 7(a–d) show the SEM images of the obtained MIP and NIP particles. It can be seen clearly that both normal and reverse ATRPP can provide MIP and NIP microspheres. The D_n values of the MIP and NIP spherical particles prepared via normal ATRPP are 3.10 and 2.99 μm, respectively, and they have a U value of 1.27 and 1.23, respectively. The D_n values of the MIP and NIP spherical particles prepared via reverse ATRPP are 3.24 and 2.70 μm, respectively, and they have a U value of 1.18 and 1.22, respectively. It is worth mentioning here that much smaller MIP and NIP spherical particles were obtained via TRPP under similar reaction conditions (with their D_n values being 266 and 273 nm, respectively, and their U values being 1.14 and 1.10, respectively; Figures not shown), similar to the above-described BPA imprinted polymer system.

The binding properties of the obtained MIPs and NIPs were then investigated with equilibrium binding experiments. The MIP microspheres prepared via both normal and reverse ATRPP proved to show higher binding capacities towards 2,4-D than their corresponding NIPs (Fig. 8). For example, in a dilute solution of 2,4-D in acetonitrile, while 22 mg of the imprinted microspheres prepared via normal and reverse ATRPP bound 49 and 43% of the template, respectively, an equivalent amount of the corresponding controls

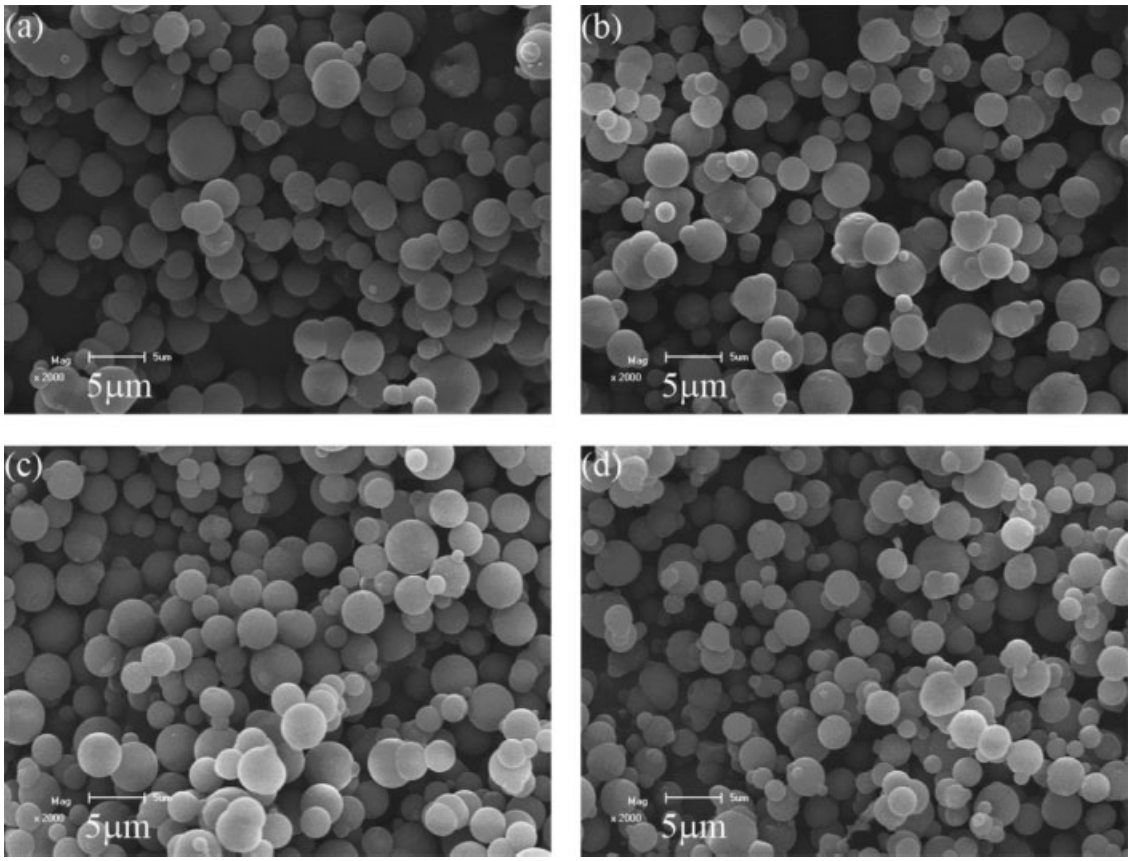

Figure 7. Scanning electron micrographs of the MIPs (template: 2,4-D) (a,c) and NIPs (b,d) prepared via normal ATRPP (a,b) and reverse ATRPP (c,d), respectively.

bound only 37 and 32%, respectively, thus confirming the successful generation of selective binding sites by 2,4-D in the obtained MIP microspheres.

The binding selectivity of the MIPs prepared via both normal and reverse ATRPP was also studied by measuring their competitive binding capacities towards 2,4-D and two structurally related compounds, DPAc and POAc (Scheme 2), which have the same functionality (i.e., the carboxyl group) but differ either in the distance between the functional group and the benzene ring or in the numbers of the halogen substitutents on the benzene ring. As can be seen clearly from Figure 9, the MIPs exhibit significantly lower binding capacities towards DPAc and POAc than towards 2,4-D, thus demonstrating the high selectivity of the MIPs towards 2,4-D.

On the basis of the above results, we can reach a conclusion that both normal and reverse ATRPP can be successfully utilized to prepare 2,4-D imprinted microspheres ($D_n \approx 3$ μm) with obvious molecular imprinting effects towards the template and an appreciable selectivity over structurally related compounds, thus demonstrating that ATRPP is a versatile and general approach for the

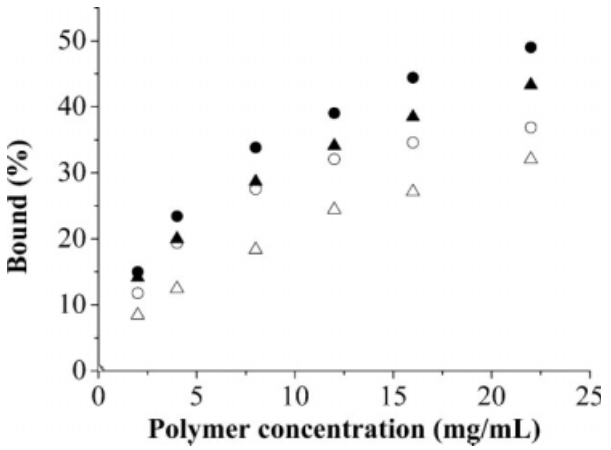

Figure 8. Equilibrium binding of 2,4-D (C = 0.08 mM) on different amounts of the MIPs (template: 2,4-D, filled symbol) and NIPs (open symbol) prepared via normal ATRPP (cycle) and reverse ATRPP (triangle), respectively.

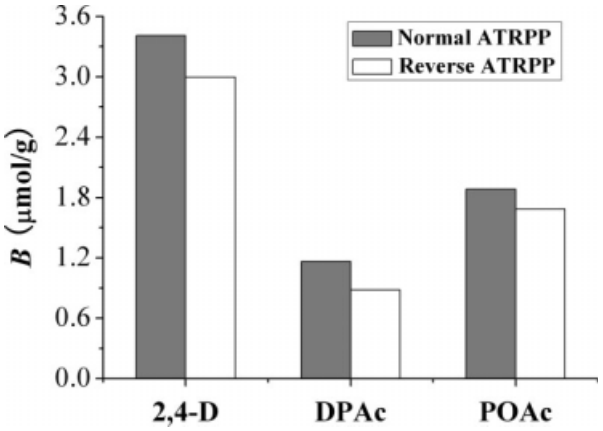

Figure 9. Selective binding of the MIPs (2,4-D as the template) prepared via normal and reverse ATRPP towards 2,4-D, DPAc and POAc in their mixed solution in acetonitrile ($C_{2,4\text{-D,DPAc or POAc}} = 0.08$ mM), respectively.

preparation of MIP microspheres for different templates.

CONCLUSIONS

We have demonstrated, for the first time, the successful application of both normal and reverse ATRPP in the molecular imprinting field. These polymerization techniques can provide MIP microspheres with obvious molecular imprinting effects towards the template, fast template rebinding kinetics and an appreciable selectivity over structurally related compounds. The unique living chain propagation mechanism in ATRPP results in MIP microspheres with much larger diameters and significantly higher high-affinity site densities in comparison with the MIP submicrospheres prepared via TRPP, thus suggesting that the application of ATRPP in the molecular imprinting field has great potential to improve the structural homogeneity and enhance the binding parameters. Besides, the general applicability of the ATRPP approach has also been demonstrated by its successful application in the preparation of 2,4-D imprinted microspheres. Considering the versatility of ATRP and the applicability of molecular imprinting to many different kinds of template molecules, we believe that ATRPP represents a simple and robust route to the preparation of functional MIP microspheres with improved binding properties. In addition, the presence of surface-immobilized reactive functional groups (i.e., the halogen group) on the obtained MIP microspheres allows their further surface modification (eventually leading to their better compatibility with different solvent systems), which makes them highly promising in many practical applications. The work in this direction is currently in progress.

The authors gratefully acknowledge the financial supports from National Natural Science Foundation of China (20744003, 20774044), Natural Science Foundation of Tianjin (06YFJMJC15100), a supporting program for New Century Excellent Talents (Ministry of Education) (NCET-07-0462) and the project-sponsored by SRF for ROCS, SEM.

REFERENCES AND NOTES

1. Wulff, G. Angew Chem Int Ed 1995, 34, 1812–1832.
2. Mosbach, K.; Ramström, O. Biotechnology 1996, 14, 163–170.
3. Sellergren, B. Molecularly Imprinted Polymers: Man made Mimics of Antibodies and Their Applications in Analytical Chemistry; Techniques and Instrumentation in Analytical Chemistry; Elsevier Science: Amsterdam, 2001; Vol. 23.
4. Haupt, K. Chem Commun 2003, 171–178.
5. Zhang, H.; Ye, L.; Mosbach, K. J Mol Recognit 2006, 19, 248–259.
6. Wang, A. R.; Zhu, S. Polym Eng Sci 2005, 45, 720–727.
7. Ide, N.; Fukuda, T. Macromolecules 1997, 30, 4268–4271.
8. Ide, N.; Fukuda, T. Macromolecules 1999, 32, 95–99.
9. Huang, W.; Baker, G. L.; Bruening, M. L. Angew Chem Int Ed 2001, 40, 1510–1512.
10. Kanamori, K.; Hasegawa, J.; Nakanishi, K.; Hanada, T. Macromolecules 2008, 41, 7186–7193.
11. Achilleos, M.; Legge, T. M.; Perrier, S.; Patrickios, C. S. J Polym Sci Part A: Polym Chem 2008, 46, 7556–7565.
12. Kato, M.; Kamigaito, M.; Sawamoto, M.; Higashimura, T. Macromolecules 1995, 28, 1721–1723.
13. Wang, J. S.; Matyjaszewski, K. Macromolecules 1995, 28, 7901–7910.
14. Percec, V.; Barboiu, B. Macromolecules 1995, 28, 7970–7972.
15. Matyjaszewski, K.; Xia, J. Chem Rev 2001, 101, 2921–2990.
16. Kamigaito, M.; Ando, T.; Sawamoto, M. Chem Rev 2001, 101, 3689–3746.
17. Zhang, H.; Jiang, X.; Van der Linde, R. Polymer 2004, 45, 1455–1466.
18. Coessens, V.; Pintauer, T.; Matyjaszewski, K. Prog Polym Sci 2001, 26, 337–377.
19. Wei, X.; Li, X.; Husson, S. M. Biomacromolecules 2005, 6, 1113–1121.

20. Li, X.; Husson, S. M. Biosens Bioelectron 2006, 22, 336–348.
21. Wei, X.; Husson, S. M. Ind Eng Chem Res 2007, 46, 2117–2124.
22. Wang, H. J.; Zhou, W. H.; Yin, X. F.; Zhuang, Z. X.; Yang, H. H.; Wang, X. R. J Am Chem Soc 2006, 128, 15954–15955.
23. Ye, L.; Cormack, P. A. G.; Mosbach, K. Anal Commun 1999, 36, 35–38.
24. Wang, J.; Cormack, P. A. G.; Sherrington, D. C.; Khoshdel, E. Angew Chem Int Ed 2003, 42, 5336–5338.
25. Yoshimatsu, K.; Reimhult, K.; Krozer, A.; Mosbach, K.; Sode, K.; Ye, L. Anal Chim Acta 2007, 584, 112–121.
26. Ye, L.; Mosbach, K. React Funct Polym 2001, 48, 149–157.
27. Storsberg, J.; Hartenstein, M.; Müller, A. H. E.; Ritter, H. Macromol Rapid Commun 2000, 21, 1342–1346.
28. Keller, R. N.; Wycoff, H. D. Inorg Synth 1946, 2, 1–4.
29. Ciampolini, M.; Nardi, N. Inorg Chem 1966, 5, 41–44.
30. Umpleby, R. J., II; Baxter, S. C.; Rampey, A. M.; Rushton, G. T.; Chen, Y.; Shimizu, K. D. J Chromatogr B 2004, 804, 141–149.
31. Zhang, H.; Verboom, W.; Reinhoudt, D. N. Tetrahedron Lett 2001, 42, 4413–4416.
32. Zhang, H.; Piacham, T.; Drew, M.; Patek, M.; Mosbach, K.; Ye, L. J Am Chem Soc 2006, 128, 4178–4179.
33. Zhang, H.; Klumperman, B.; Ming, W.; Fischer, H.; Van der Linde, R. Macromolecules 2001, 34, 6169–6173.
34. Zhang, H.; Schubert, U. S.; Chem Commun 2004, 858–859.
35. Zhang, J. H.; Jiang, M.; Zou, L.; Shi, D.; Mei, S. R.; Zhu, Y. X.; Shi, Y.; Dai, K.; Lu, B. Anal Bioanal Chem 2006, 385, 780–786.
36. Jiang, M.; Zhang, J. H.; Mei, S. R.; Shi, Y.; Zou, L. J.; Zhu, Y. X.; Dai, K.; Lu, B. J Chromatogr A 2006, 1110, 27–34.
37. Surugiu, I.; Ye, L.; Yilmaz, E.; Dzgoev, A.; Danielsson, B.; Mosbach, K.; Haupt, K. Analyst 2000, 125, 13–16.
38. Koprinarov, I.; Hitchcock, A. P.; Li, W. H.; Heng, Y. M.; Stöver, H. D. H. Macromolecules 2001, 34, 4424–4429.
39. Li, W. H.; Stöver, H. D. H. J Polym Sci Part A: Polym Chem 1998, 36, 1543–1551.
40. Boonpangrak, S.; Whitcombe, M. J.; Prachayasittikul, V.; Mosbach, K.; Ye, L. Biosens Bioelectron 2006, 22, 349–354.
41. Pérez-Moral, N.; Mayes, A. G. Macromol Rapid Commun 2007, 28, 2170–2175.
42. Watabe, Y.; Hosoya, K.; Tanaka, N.; Kubo, T.; Kondo, T.; Morita, M. J Chromatogr A 2005, 1073, 363–370.
43. Vaughan, A. D.; Sizemore, S. P.; Byrne, M. E. Polymer 2007, 48, 74–81.
44. Haupt, K.; Dzgoev, A.; Mosbach, K. Anal Chem 1998, 70, 628–631.